LIGHT SCATTERING STUDIES OF A MODEL ELECTRORHEOLOGICAL FLUID

THOMAS C. HALSEY

The James Franck Institute and Department of Physics
The University of Chicago
5640 South Ellis Avenue
Chicago, Illinois 60637

and

JAMES E. MARTIN

Advanced Materials Physics Division
Sandia National Laboratories
Albuquerque, New Mexico 87185

ABSTRACT

Electrorheological suspensions typically contain particles of approximately one μm in diameter. Thus light-scattering offers a natural method of probing the microstructure of these suspensions. We report the development of an index matched single-scattering fluid, as well as light-scattering studies of this fluid in both a quiescent and sheared regime. In the first case, the results are in agreement with a phenomenological theory of coarsening based on thermal fluctuations. In the second case, they agree with an "independent droplet" model of the suspension structure under shear.

1. Introduction

In unravelling the microstructure of electrorheological (ER) suspensions, light scattering is potentially a very useful tool. This is due to the happy accident that the typical size of the suspended particles in such a fluid is comparable to the wavelength of light.[1] Thus single-scattering of light from an ER suspension will yield direct and easily interpretable information about its structure, under any flow conditions.

Unfortunately, most commercial and experimental ER fluids have particles with dielectric constants at optical frequencies significantly different from the surrounding liquid. Thus these fluids are in a multiple-scattering regime for light. This property has been used by Ginder and Elie[2] to extract structural information, but the potential of multiple-scattering techniques is limited by difficulties of interpretation.

For this reason, we developed a model ER fluid with particles whose index of refraction was closely matched to that of the surrounding liquid.[3] While probably not useful for applications, this fluid is an excellent laboratory for the study of ER fluid microstructure.

So far we have addressed two physical questions with this fluid. The first is the nature of the solidification transition of an ER suspension when a field is applied. Since the original observations of Winslow, many observers have noted the appearance of fibrous structures, often one particle thick, parallel to the applied field.[1,4] However, recent theories predict that the ultimate high-field state of an ER suspension will be a phase separated solid, rather than a set of widely dispersed fibers or particle chains.[5,6] Our results bridge this apparent contradiction by showing that, while it is true that the original state of the ER fluid after the application of a field consists of thin chains of particles aligned with the field, these fibers slowly drift together in the direction transverse to the field, forming columns of larger and larger diameter. The end product of this process will clearly be the phase-separated colloidal solid beloved of theorists. A phenomenological theory based upon the idea that the thermal fluctuations of the chains catalyze this "coarsening" process accounts well for the quantitative details of this process.[3,7].

In a shear flow, there are two competing models of the microstructure. Klingenberg and Zukoski accounted for the Bingham plastic response of the suspensions by postulating (and observing) that boundary layers of ER ordering formed near the electrodes, which were melted some way into the fluid by the shear flow.[8] Halsey, Martin, and Adolf have proposed a different mechanism, in which the electrodes play no special role, but "droplets" of condensed particles form throughout the fluid.[9] The size of these droplets is then fixed by a balance between electrical and hydrodynamical forces. We have studied the microstructure in the interior of a sheared ER fluid, and have found evidence for the existence of such droplets, and of such a balance. Of course, this does not exclude the possibility that Klingenberg-Zukoski boundary layers may form closer to the electrodes.

In this chapter, we will first report details of the synthesis of our model fluid. We will then report our experimental results in the two areas mentioned above, and briefly compare them with theory.

2. Sample Preparation

The colloids in our model fluid are synthesized by the base-catalyzed nucleation and growth of monodisperse silica spheres from tetraethoxysilicon. To reduce the Keesom interactions that lead to aggregation, this synthesis was conducted in mixed organic solvents that index-match the growing spheres. Scanning electron microscopy and elastic and quasielastic light scattering measurements indicate that 0.7 μm diameter silica spheres are easily formed at high silica concentrations under mild hydrolysis with 0.5M NH_4OH. The elastic light scattering data are consistent with a Gaussian sphere radius r_d distribution having σ_{r_d}/r_d of 10.5%. The

hydrophilic silica spheres were then coated with the organophilic silane coupling agent 3-'trimethoxysilyl' propyl methacrylate via a condensation reaction.[10] After a 24-hour vacuum distillation of water and ammonia, the spheres were centrifuged at low acceleration, the supernatant decanted, and the soft colloidal solid was redispersed in 4-methylcyclohexanol, again chosen to closely index match the spheres. The two samples used in this study measure 20 wt % and 34 wt % by thermal gravimetric analysis, although the high concentration sample was diluted to 11 wt % for the kinetics studies. The refractive index increment of $dn/dc = 0.0017$ ml/g is small enough to insure single scattering from concentrated dispersions; indeed, depolarization of the scattered light was negligible.

To measure the surface charge of the colloids, electrophoresis measurements were made with a Pen Kem Laser Zee^{TM} apparatus. Since we were unable to observe any electrophoresis with this apparatus we simply applied a 1 kV/mm electric field to the particles and observed their behavior through a Nikon Microphot-FXA^{TM} optical microscope. Even at these high electric fields we were unable to observe electrophoresis of these particles, although at high applied frequencies field-induced particle chaining was observed and was found to be reversible by Brownian motion alone.

3. Quiescent Fluid Studies

3.1 Experimental Results

Representative scattering data taken after an electric field quench, shown in Figure 1, clearly indicate an unstable concentration fluctuation orthogonal to the electric field lines in the fluid. This corresponds to the formation of chains of particles parallel to the field. This scattering pattern dissipates immediately when the field is turned off, indicating that structure formation is perfectly reversible in this fluid.

Figure 1. The scattered intensity from an electrorheological fluid shortly after the application of a strong electric field. The lobes appear at scattering wavevectors orthogonal to the electric field, indicating the appearance of chains of particles parallel to the electric field.

The evolution of the scattering intensity, or structure factor, in the direction perpendicular to the field is shown in the inset to Figure 2. This corresponds to a slice through the lobe shown in Figure 1. It is clear that as time progresses, the peak increases in intensity and moves to smaller values of wave-vector $q_\perp$ in the direction perpendicular to the field. This corresponds to the slow agglomeration of chains into columns. By dividing the intensity by the peak intensity I_{max}, and dividing the scattering wave vector by the peak wave vector $q_{\perp,max}$, we are able to demonstrate that the evolving structures scale, as evinced by the data collapse in Figure 2.

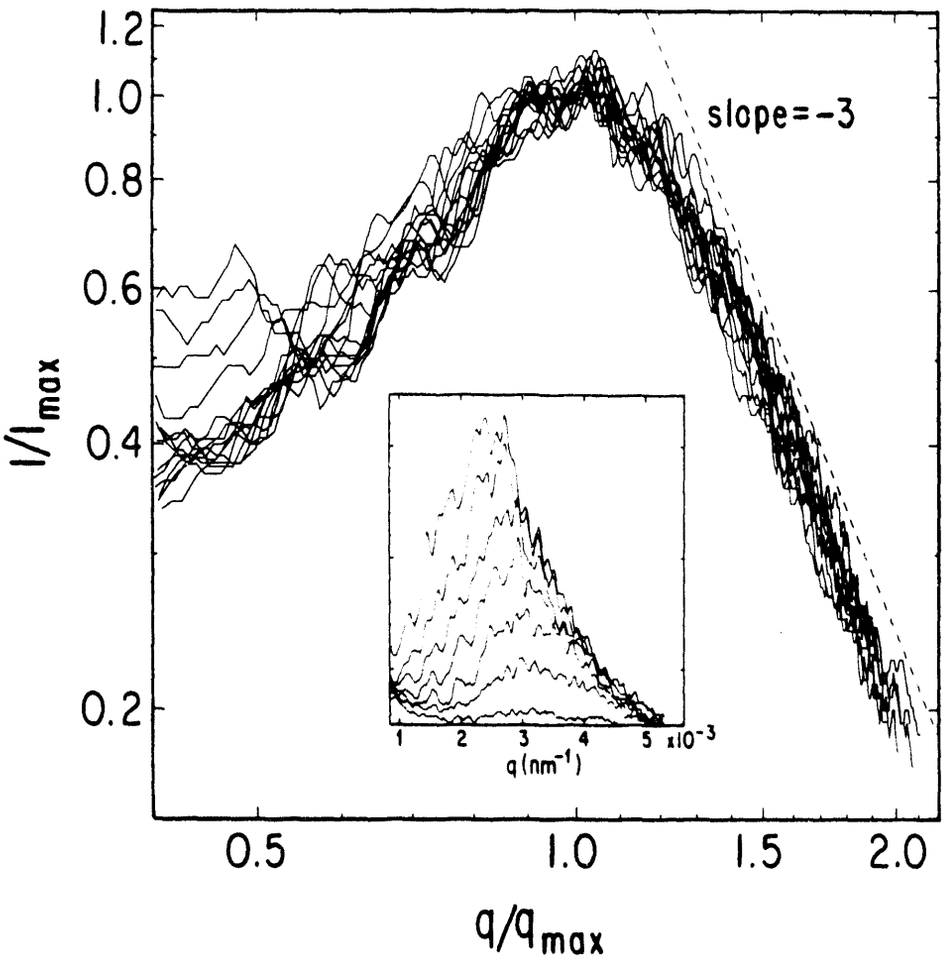

Figure 2. The inset shows intensity slices through one lobe of the scattering pattern in Figure 1 for various times. As time increases the peak intensity increases and moves to larger length scales (smaller q), corresponding to the agglomeration of chains of particles into columns. When the intensity data are plotted on dimensionless axes a master curve results, indicating scaling. On the high-q side of the peak the data fall off as q^{-3}, which indicates that the column surfaces are sharp.

These scattering data have a high-q shoulder that decays as q^{-3}. This is Porod's law in two dimensions, and indicates that the structures have sharp, non-fractal interfaces in the direction perpendicular to the field.[11] This is consistent with the picture that the agglomerating chains form compact columns. Finally, a $\log - \log$ plot shows that $I_{max} \propto q_{\perp,max}^{-2.25}$, which suggests that within experimental error the scattering intensity $I(q_\perp, t)$ obeys

$$I(q_\perp, t) \approx q_{\perp,max}(t)^{-d} f(q/q_{\perp,max}(t)) \qquad f(x) \propto x^{-(d+1)} \tag{1}$$

with $d = 2$, corresponding to the essentially two-dimensional nature of the coarsening process.

It remains to discuss the behavior of $q_{\perp,max}(t)$. In order to reduce the noise in the signal, we used the moments

$$I_k(q_l, q_m) = \int_{q_l}^{q_m} q^k I(q) dq \tag{2}$$

In practice, the lower integration limit $q_l = 0.33 \times 10^{-3}\text{nm}^{-1}$ is determined by the size of the beam stop, while the upper limit $q_m = 0.529 \times 10^{-2}\text{nm}^{-1}$ is set by the camera position. The wave vector of peak intensity can now be obtained from the ratio of I_1 to I_0.

The time dependence of the characteristic length scale (or inter-column spacing) $\tilde{R}(t) = 2\pi/q_{\perp,max}(t)$ is shown in Figure 3 for peak to peak voltages of 0.56 kV/mm, 1.25 kV/mm, and 2.6 kV/mm. At the earliest times, the characteristic length is $\tilde{R}(0) \approx 1.9\mu$m. At later times, $\tilde{R}(t)$ is observed to increase approximately as $t^{0.42}$. In the spinodal decomposition of systems with a "conserved order parameter", such as binary alloys, there is typically an intermediate time regime ("Lifshitz-Slyozov ripening") in which a characteristic length scale of the structure increases as $t^{1/3}$.[12] Thus the ER fluid coarsening is anomalously fast by comparison with ordinary spinodal decomposition; presumably this is a reflection, in some way, of the importance of long-ranged forces in this system.

However, we cannot account for this coarsening by postulating some simple mechanism of dipolar interaction between adjacent chains or columns. Any such mechanism will involve forces $\propto E^2$ acting on particles which feel a viscous drag $\propto \mu_0$, where μ_0 is the dispersing fluid viscosity. This latter assumes (reasonably) that the hydrodynamics of particle motion is in the low-Reynolds number limit. Thus we expect that the characteristic time scale t_c for electrostatically-driven coarsening would be $t_c \propto \mu_0/E^2$. However, it is clear from Figure 3 that in our experiments, t_c depends much more weakly upon E; our actual result for the three electric fields

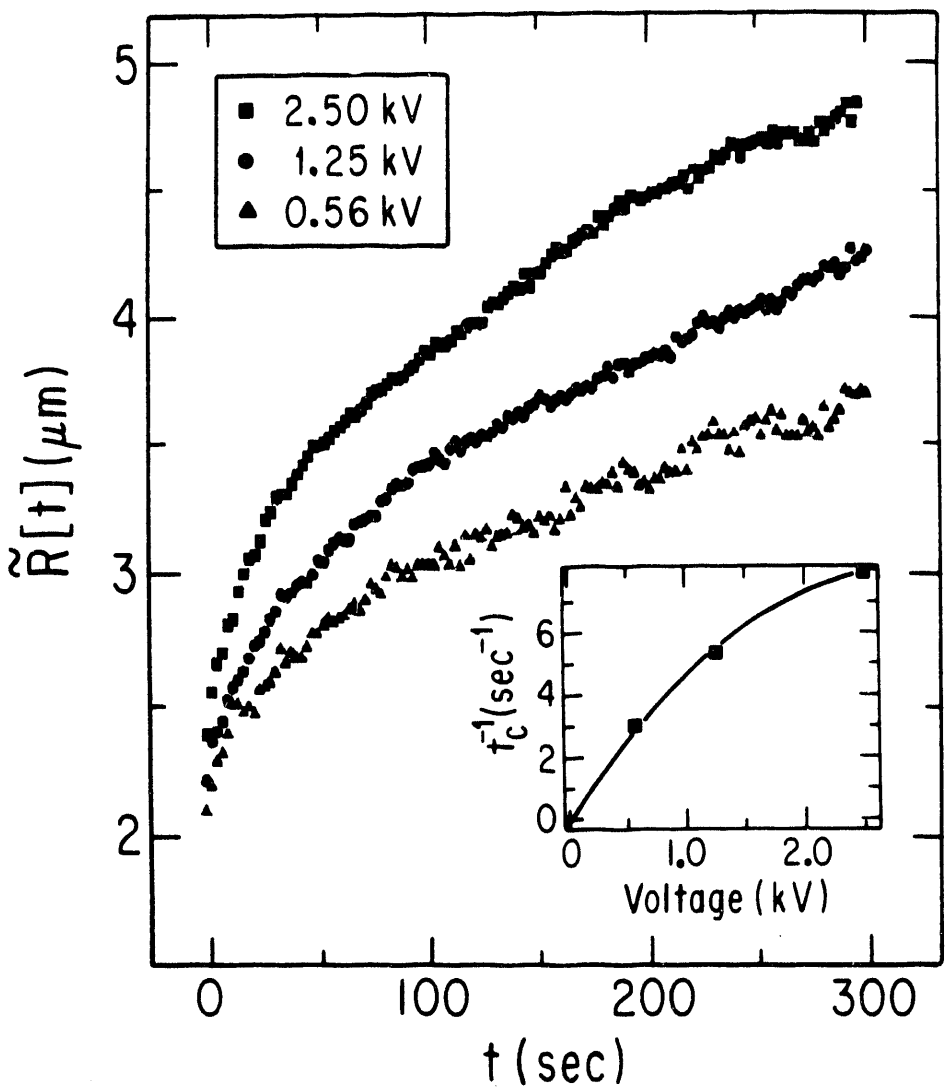

Figure 3. The distance between columns in a quiescent fluid increases as $\tilde{R}(t) = \tilde{R}(0)[1+(t/t_c)^{0.42}]$. The inset shows the increase of the growth rate t_c^{-1} with electric field. The fact that t_c^{-1} is not $\propto E^2$ implies that the coarsening is not driven simply by dipolar forces.

used is $t_c \propto E^{-0.6}$. Thus, from dimensional analysis alone, we conclude that some other energy scale must be involved in determining the coarsening process.

Since the initial structure formation parallel to the electric field does occur on a time scale $t_a \propto \mu_0/E^2$, as demonstrated, e.g., by Ginder and Elie,[2] this implies that the structure formation parallel and perpendicular to the field are driven by different mechanisms on different time scales, the latter being a much slower process.

This two-step process of structure formation was first predicted by Halsey and

Toor.[5] On a time scale determined by t_a, chains or columns of particles, whose diameter at high fields will be at most a few particles, will form parallel to the field. At high fields, this initial aggregation phase should be dominated by the ballistic motion of particles into these chain-like aggregates; the aggregates will remain one-dimensional due to their tendency to aggregate predominantly at their ends. The one-dimensional structures obtained are not the true ground state of the suspension. However, the further relaxation of these chains by motion perpendicular to the field into columnar structures is not driven by the simple electrostatic attraction of parallel chains, as this attraction is quite short-ranged.

3.2 Theoretical Results

We have proposed that the mechanism by which the chains move together is related to the thermal fluctuations of the internal configuration of a chain.[13] The importance of thermal, or Brownian effects, in ER fluids is generally expressed by a dimensionless group λ, which is defined as[14]

$$\lambda = \frac{\pi \epsilon_0 \epsilon_s (\beta E)^2 r_d^3}{k_B T}, \tag{3}$$

where ϵ_s is the dispersing fluid dielectric constant, β is the particle polarizability, k_B is Boltzmann's constant, and T is the temperature. Typically, experiments on ER effects, including ours, have been conducted at quite high values of $\lambda \sim 10^{4-5}$. Thus the proposition that thermal effects might be important, in this regime where polarization energies are very much larger than $k_B T$, is quite counter-intuitive. However, because the interactions between perfect, zero-temperature chains are negligible if they are separated by distances greater than the intra-chain distance between particles, any long-ranged force arising from thermal effects, even if quite weak, might be significant in the long-time behavior of these suspensions.

In calculating the effect of the thermal fluctuations on the positions of particles in the chains, two possible assumptions are possible regarding the relevant time scales. The time scale over which thermal fluctuations relax defines t_f, which may be larger or smaller than the typical transverse coarsening (column formation) time t_c. If $t_f \ll t_c$, then the fluctuations of parallel chains give rise to an interaction of Van der Waals form,

$$F(\rho) = -A \frac{k_B T r_d^4 L}{\rho^5} \tag{4}$$

where $F(\rho)$ is the free energy of interaction of two parallel chains of length L, separated by a distance ρ, and A is a (large) numerical constant. For typical ER fluids, this attractive interaction would lead to coarsening with a time scale $t_c \sim 100$ sec.

On the other hand, if $t_f \gg t_c$, then a much stronger interaction between chains results. A simple scaling estimate yields

$$t_c \sim t_a \lambda^{3/5} \left(\frac{\tilde{R}(t)}{r_d} \right)^{9/5} \tag{5}$$

which determines how the coarsening time depends both on the developing distance between chains (or columns) $\tilde{R}(t)$, as well as its dependence on the electric field through λ. The coarsening predicted by Eq. (5) is in fairly good agreement with our experimental results, as it predicts that $\tilde{R}(t) \propto t^{5/9}$ and $t_c \propto E^{-4/5}$, compared to experimental exponents of 0.42 and -0.6, respectively. However, in the absence of a convincing microscopic derivation of t_f, the fluctuation approach must be regarded as only phenomenological.

This approach accounts at least qualitatively for the dependence of column formation on colloid volume fraction ϕ_c. We observed that the initial length scale $\tilde{R}(0)$ decreased with increasing concentration, but the growth rate increased. This is reasonable because we expect that $\tilde{R}(0) \propto \phi_c^{-1/2}$ in an initial array of parallel chains, and closer chains will feel a greater fluctuation-induced attraction, and thus coarsen into columns more quickly.

4. Steady Shear Studies

Our interest in shear stems from some unusual results we reported for the shear thinning viscosity of our model ER fluid.[9] In particular, we found that when the shear rate $\dot{\gamma}$ was increased, the suspension viscosity decreased as $\mu_s \propto \dot{\gamma}^{-\Delta}$, with $\Delta \approx 2/3$, at least at lower applied fields. Although qualitatively similar to the much observed "Bingham plastic" behavior, this behavior is quite different in detail from that of a Bingham plastic.

To see this, consider the shear stress τ_{xy}. In the Bingham plastic model, $\tau_{xy} = \tau_0 + \mu_\infty \dot{\gamma}$, where τ_0 is the yield stress and μ_∞ is the infinite shear rate viscosity. Thus the Bingham plastic has a constant differential viscosity $d\tau_{xy}/d\dot{\gamma} = \mu_\infty$. However, our results showed a differential viscosity $d\tau_{xy}/d\dot{\gamma} \propto \dot{\gamma}^{1-\Delta}$ which went to zero at low shear rates.

In collaboration with D. Adolf, we proposed a model for this behavior, the "independent droplet" model, in Ref. 9. This model is based upon an analysis of the response of an individual condensed droplet of dielectric particles to the combined effect of an electric field and a hydrodynamic flow. This droplet should be imagined to consist of a large number of individual colloidal particles, condensed into some ordered structure.

Suppose that the vorticity of the hydrodynamical flow is perpendicular to the electric field. Then a droplet of particles elongated in the field direction will feel a

torque, which will tend to rotate it in the same sense as the hydrodynamic vorticity. However, once the long axis of such a droplet is rotated away from the electric field direction, it feels a restoring torque due to the electric field. If one restricts oneself to ellipsoidal droplets, both the electrical and the hydrodynamical torques are known exactly. For a prolate spheroidal droplet of minor radius b and major radius c, the hydrodynamical torque L obeys[15]

$$L \sim \mu_0 V \dot{\gamma} \frac{c^2}{b^2} \tag{6}$$

where V is the droplet volume. The electrical torque is given by a standard formula, which depends upon the depolarization factors of the ellipsoid.[16]

Note that we implicitly assume that the polarization of the individual particles is always parallel to the local electric field, so that the electrical torque arises from the interaction among the different particles in the droplet. This is in contrast to the work of Hemp,[17] who studied individual particles whose polarization lagged the local electric field in time by some phase; these particles can contribute an electrorheological effect without the need for significant inter-particle interactions.

For any particular droplet, the angle θ that the droplet axis makes with the electric field direction can be calculated as a function of the Mason number $\mathrm{Mn} = (6\mu_0\dot{\gamma}/\epsilon_0\epsilon_s(\beta E)^2)$. In addition, θ is a function of the aspect ratio of the droplet, the ratio of the large radius c to the small radius b. The result is

$$\theta \sim \mathrm{Mn}(c/b)^2 \tag{7}$$

so that longer droplets are rotated by a larger angle away from the field direction. In so doing, they lose much of their favorable depolarization energy. Thus a hydrodynamical flow field will tend to reduce the size of structures in an ER suspension.

An actual suspension will, of course, consist of many such droplets, which will collide with one another as well as break up under the influence of the flow. One might thus expect that the typical size of droplets in a flow will be set by the maximum stable size of a droplet, because droplets below this size which collide will tend to aggregate, while droplets above this size will break up. There are two sources of polarization energy for a droplet. The first is the depolarization energy at the equilibrium angle, as determined by the two competing torques mentioned above. The second effect is the surface energy of a droplet.[18] Balancing these two effects, one finds that

$$\begin{aligned} c &\propto \mathrm{Mn}^{-1} \\ b &\propto \mathrm{Mn}^{-2/3} \end{aligned} \tag{8}$$

Figure 4. The scattering pattern of a sheared fluid is rotated with respect to that of a quiescent fluid (Figure 1). In this case, the shear rate $\dot{\gamma} = 1.04\text{s}^{-1}$. There is also a much stronger intensity near the origin, where the scattering wave-vector is small, than for the quiescent fluid.

which sets the length and width of droplets. This implies that θ is given by

$$\theta \propto \text{Mn}^{1/3} \tag{9}$$

and that the macroscopic suspension viscosity scales as

$$\mu_s \propto \text{Mn}^{-2/3} \tag{10}$$

Since $\text{Mn} \propto \dot{\gamma}$, this result is in agreement with the low-field experimental results mentioned above.

In our light-scattering studies, we first applied an electric field to a quiescent fluid. When a steady shear was then applied to the sample, the scattering pattern rotated in the direction of the vorticity and the maximum intensity of the scattering lobes moved to $q = 0$, as shown in Figure 4. After a brief period, the scattering intensity no longer changed with time.

These results can be interpreted in terms of the existence of some sort of rotated structures in the fluid, be they droplets or un-fragmented columns. To proceed further, we analyze the angular distribution of the scattering pattern, and in particular the angle of its maximum $\tilde{\theta}_{max}$, as a function of $\dot{\gamma}$. It is natural to identify this angular maximum position with θ from Eq. (7), the angle a droplet makes to the electric field.

To determine $\tilde{\theta}_{max}$, we first divided a time-averaged scattering image into 360 wedges, each subtending 1° of arc. We then integrated the total intensity in each wedge, and plotted the result versus angle. The maximum of such a plot determines

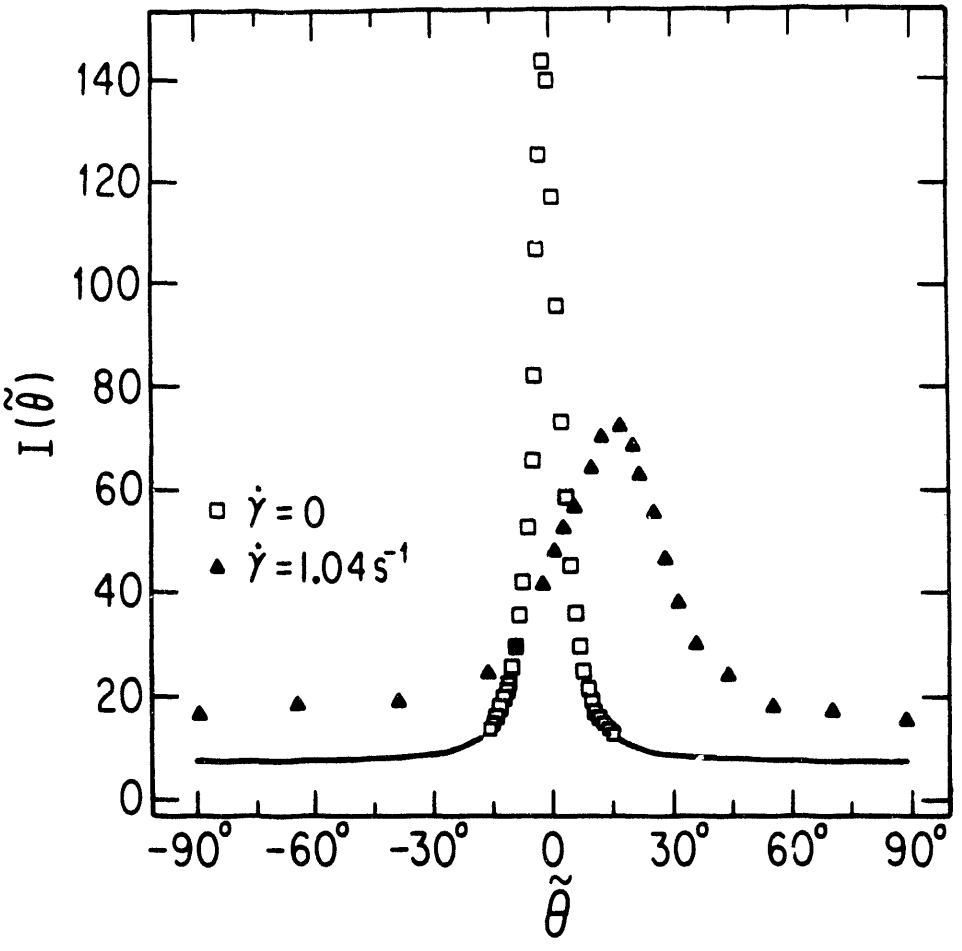

Figure 5. "Pie-o-metric" analysis indicates the angular distribution of the scattered light in quiescent and sheared fluids. Lobes perpendicular to the field, as in Figure 1, give an angular distribution sharply peaked about the direction perpendicular to the field ($\tilde{\theta} = 0$). In a sheared fluid with $\dot{\gamma} = 1.04s^{-1}$, the lobes are broader and are also rotated.

$\tilde{\theta}_{max}$. We have coined the term "pie-o-metric analysis" to describe this procedure, because it lends this somewhat arbitrary method a certain cachet otherwise lacking. Figure 5 compares the result of this procedure for a quiescent fluid with that for a fluid sheared at a rate of $\dot{\gamma} = 1.04s^{-1}$. The sheared result is considerably broader, but nevertheless has a clearly identifiable peak.

The dependence of $\tilde{\theta}_{max}$ on $\dot{\gamma}$ is shown in Figure 6. The least squares fit to the exponent gives

$$\theta_{max} \propto \dot{\gamma}^{\delta} \quad \delta = 0.326 \tag{11}$$

in superb agreement with the prediction $\delta = 1/3$ from Eq. (10). Note that if the structures did not fragment with increasing shear rate, Eq. (8) would predict $\delta = 1$, which is certainly excluded. Our results thus vividly demonstrate the fragmentation of the droplets as the shear rate is increased, and provide independent confirmation for the independent droplet model.

5. Conclusions

In this chapter, we have explored two different problems in the "semi-dilute" ER fluid regime. In each case, the dipolar interactions of the particles give rise to novel physics on intermediate length scales. For the problem of the coarsening of a quiescent fluid, our experimental results can be at least partially understood

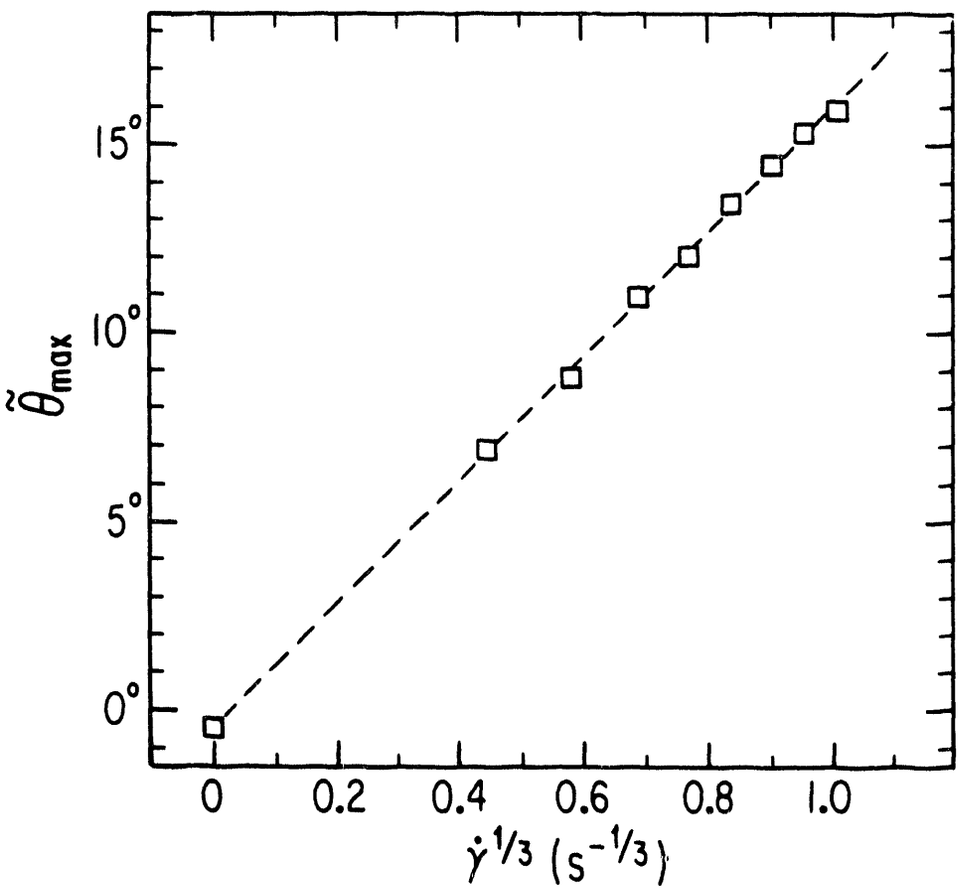

Figure 6. The maximum of the angular pattern from Figure 5, $\tilde{\theta}_{max}$, graphed versus the shear rate $\dot{\gamma}^{1/3}$. The linearity of this plot is strong evidence for the "independent droplet" model, which claims that droplets are rotated by an angle $\theta \propto \dot{\gamma}^{1/3}$ from the electric field direction.

as arising from a thermal fluctuation mechanism. Our understanding in the sheared fluid seems, at this stage, to be more complete. A model of fragmenting and recombining droplets, which was originally devised to account for the macroscopic rheological respone of the fluid, is also in excellent agreement with light-scattering observations of the fluid microstructure.

6. Acknowledgements

The work discussed in this chapter was performed in collaboration with D. Adolf, J. Odinek, and W. Toor. T.C.H. is grateful to the National Science Foundation for the support of this research through the Presidential Young Investigators program, grant DMR-9057156. Acknowledgement is made to the Donors of The Petroleum Research Fund, administered by the American Chemical Society, for the partial support of this research. The work of J.E.M. was performed at Sandia National Laboratories and was supported by the U.S. Department of Energy under Contract No. ED-AC04-76DP00789.

References

1. A.P. Gast and C.F. Zukoski, *Adv. Colloid Interface Sci.* **30** (1989) 153.
2. J.M. Ginder and L.D. Elie, in *Proceedings of the Conference on Electrorheological Fluids* ed. R. Tao (World Scientific, Singapore, 1992).
3. J.E. Martin, J. Odinek, T.C. Halsey, *Phys. Rev. Lett.* **39** (1992) 1524.
4. W. Winslow, *J. Appl. Phys.* **20** (1949) 1137.
5. T.C. Halsey and W. Toor, *Phys. Rev. Lett.* **65** (1990) 2820.
6. R. Tao and J.M. Sun, *Phys. Rev. Lett.* **67** (1991) 398; *Phys. Rev. A* **A44** (1991) R6181 . For an elegant experimental confirmation, see T.-j. Chen, R.N. Zitter, R. Tao, *Phys. Rev. Lett.* **68** (1992) 2555.
7. T.C. Halsey and W.R. Toor, *J. Stat. Phys.* **61** (1990) 1257; W.R. Toor, *J. Coll. Interface Sci.* **153** (1993) 335 .
8. D.J. Klingenberg and C.F. Zukoski, *Langmuir* **6** (1990) 15.
9. T.C. Halsey, J.E. Martin, D. Adolf, *Phys. Rev. Lett.* **68** (1992) 1519; and unpublished. A similar model was introduced for "magneto-rheological" fluids by Z.P. Shulman, V.I. Kordonsky, E.A. Zaltsgendler, I.V. Prokhorov, B.M. Khusid, and S.A. Demchuk, *Int. J. Multiphase Flow* **12** (1986) 935.
10. A.P. Philipse and A. Vrij, *J. Coll. Interface Sci.* **128** (1987) 121.
11. G. Porod, *Kolloid-Z.* **124** (1951) 83; **125** (1952) 51, 109.
12. E.M. Lifshitz and L.P. Pitaevski, *Physical Kinetics* (Pergamon Press, New York, 1981) p. 432-8.

13. For a review, see T. C. Halsey, *Science* **258** (1992) 713.

14. P.M. Adriani and A.P. Gast, *Phys. Fluids* **31** (1988) 2757.

15. G.B. Jeffery, *Proc. Roy. Soc. (London)* **A102** (1922) 161.

16. L.D. Landau, E.M. Lifshitz, and L.P. Pitaevski, *Electrodynamics of Continuous Media, 2nd ed.* (Pergamon Press, New York, 1984) p. 42.

17. J. Hemp, *Proc. R. Soc. Lond.* **A434** (1991) 297.

18. W.R. Toor and T.C. Halsey, *Phys. Rev.* **A45** (1992) 8617.

DATE
FILMED
4/25/94
END